C146-E268

SHIMADZU
Excellence in Science

Technical Report

Structural Analysis of Glycosphingolipids by LC-IT-TOF-MS

Akemi Suzuki[1], Jin-ichi Inokuchi[2], Masakazu Nagafuku[2], Hideshi Fujiwake[3], Yoshikatsu Umemura[3]

Abstract:

A method for detection and structural characterization of glycosphingolipids (GSLs) based on LC-IT-TOF-MS is introduced and the results of analysis of GSLs containing sialic acid in mouse thymocytes, CD4T and CDT8 cells are described as an example of its application. Even at trace levels and in a mixture, both carbohydrate chain and lipid structures were characterized, and previously unknown information could be obtained. The development of new analytical tool is in progress and applicable future challenges are discussed.

Keywords: LC-IT-TOF-MS, glycosphingolipids, gangliosides, mouse T cells, microdomain

1. Introduction

Glycosphingolipids (GSLs) are composed of a carbohydrate chain and a lipid, and localized at the cell membrane. The lipid part interacts with other membrane components and anchors the GSL at the cell membrane, and the carbohydrate chain protrudes from the cell. The carbohydrate chains are recognized by carbohydrate-recognition molecules, and are responsible for a variety of biological functions, such as cell-cell recognition, signaling, adhesion of bacteria and viruses, and binding of toxins, etc. Research for functions carried out by the sugar chains of glycoproteins can be directed by identification of the core protein, but that for GSLs require identification of membrane molecules interacted directly with GSLs in the membrane. It is easy to imagine that identification of the protein portion of the glycoprotein is essential for functional analysis, but this could not be simply extended to GSLs. The lipid raft concept proposed by K. Simons et al. in 1997 to characterize molecular interaction in the cell membrane resonated widely among researchers(1). It is the concept that the cell membrane is non-uniform and consists of many types of fine structures referred to as rafts which function as moving platforms within a fluid bilayer. It is believed that the authors' hypothesis is correct that many types of fluid microenvironments, referred to as microdomains, exist and hold membrane function proteins as scaffolding. However, we herein offer a more comprehensive definition of this microdomain as a microenvironment that includes functional molecules, lipid molecules that tightly and specifically interact with the functional molecules, and less tightly interacting lipid molecules around these complexes. The challenge now is to obtain experimental results which prove the correctness of this hypothesis.

Under such circumstances, it is believed that conducting structural analysis of GSLs by LC-IT-TOF-MS (liquid chromatography-ion trap-time of flight-mass spectrometry) may result in a major turning point in the functional analysis of GSLs. Up to now, it is possible to characterize sugar chain structures by lectins, antibodies, and sugar chain recognition molecules at trace levels, but the structure of the lipid moiety was not accessible and nearly unmanageable. Then, commercially available purified GSLs contain a uniform sugar chain, but a mixture of lipid components, and such GSLs were used for experiments of functional analysis of GSLs. Using a trace level biological sample in the mixture, characterization not only of the sugar chain structure but the lipid structure as well becomes possible by LC-IT-TOF-MS. Understanding of the partner molecules that GSLs interact with via hydrophobic interaction possibly makes GSL functions clear.

2. Structure of GSLs

Here, we describe the structure and designation of GSLs. Referring to Fig. 1, biosynthesis of GSLs starts from the lipid component. C18 3-ketosphinganine is produced from C16 palmitoyl CoA and serine, and the carbonyl group is reduced to biosynthesize sphinganine. The fatty acid is transferred by ceramide synthase from acyl CoA to the amino group to create dihydroceramide. Here, mainly even-numbered saturated fatty acids from C16:0 to C24:0 are transferred. The fatty acid chain length is determined by the substrate specificity of multiple ceramide synthases. For some reason, the C23:0 odd-chain number fatty acid and C24:1 unsaturated fatty acid are also transferred, and are detected as major structural components in biological materials. While it is known that ceramide plays an important role in the formation of water barrier in the skin, very long chain C30 fatty acids are incorporated in the skin ceramide, and the ω terminal is hydroxylated.

The insertion of a double bond in the C4-5 position of sphinganine in dihydroceramide, through the action of the desaturation enzyme referred to as Des1, produces a ceramide which contains sphingenine. On the other hand, when a hydroxyl group is introduced into the C4 position of sphinganine by the hydroxylase referred to as Des2, 4-hydroxyceramide or phytoceramide is created. A glucosylceramide (GlcCer), in which glucose (Glc) has been transferred to ceramide, can be written as GlcCer(d18:1-16:0). This expresses a structure in which a C16 saturated fatty acid is bound to C18 sphingenine via an acid amide bond. The "d" of d18:1 is used to indicate that sphingenine possesses two hydroxyl groups, that one of them is used for attachment of a sugar chain, and that the double bond is between C4-5. GlcCer consisting of sphinganine or dihydrosphingosine and C16 fatty acid is written as GlcCer(d18:0-16:0).

1 Institute of Glycoscience, Tokai University
2 Institute of Molecular Biomembrane and Glycobiology, Tohoku Pharmaceutical University
3 Analytical & Measuring Instruments Division, Shimadzu Corporation

Sugar chains are created via one-by-one addition of simple sugars, being catalyzed by glycosyltransferases. If galactose (Gal) is added to Cer, a sialic acid-added GM4 (NeuNAcα3Galβ1Cer) and sulfate group-added sulfatide (SM4: SO3 3Galβ1Cer) are formed, but further elongation of the sugar chain does not occur. This is because enzyme genes responsible for sugar chain elongation were, for some reason, not created during the evolutionary process. If glucose (Glc) is added to Cer, further elongation occurs. The Gal addition forms Galβ4Glcβ1Cer (LacCer), and from there, the NeuNAc addition produces NeuNAcα3Galβ4Glcβ1Cer (GM3), one of gangliosides, the Gal addition Galα4Galβ4Glcβ1Cer, a globo-series GSL, the N-acetylglucosamine (GlcNAc) and Gal additions, Galβ4GlcNAcβ3Galβ4Glcβ1Cer, a neolacto-series GSL, and Galβ3GlcNAcβ3Galβ4Glcβ1Cer, a lacto-series GSL. In this paper, we introduce the structural analysis of GSLs containing sialic acid, gangliosides. Fig. 1 shows the ganglioside biosynthetic pathways focusing on the molecules of interest.

Ganglioside is the generic name of GSLs containing sialic acid, but there are 3 types of sialic acid based on skeletal structure, N-acetylneuraminic acid (Neu5Ac or NeuNAc), N-glycolylneuraminic acid (Neu5Gc or NeuNGc), and keto-deoxynononic acid (Kdn). NeuNAc is the principal type of sialic acid in humans and NeuGc is barely expressed due to the deficient production of NeuNGc by mutated enzyme gene. Mammals other than humans, up to and including chimpanzees, do express NeuNGc. Here, we introduce our analysis of mouse T lymphocyte gangliosides containing NeuNGc[2].

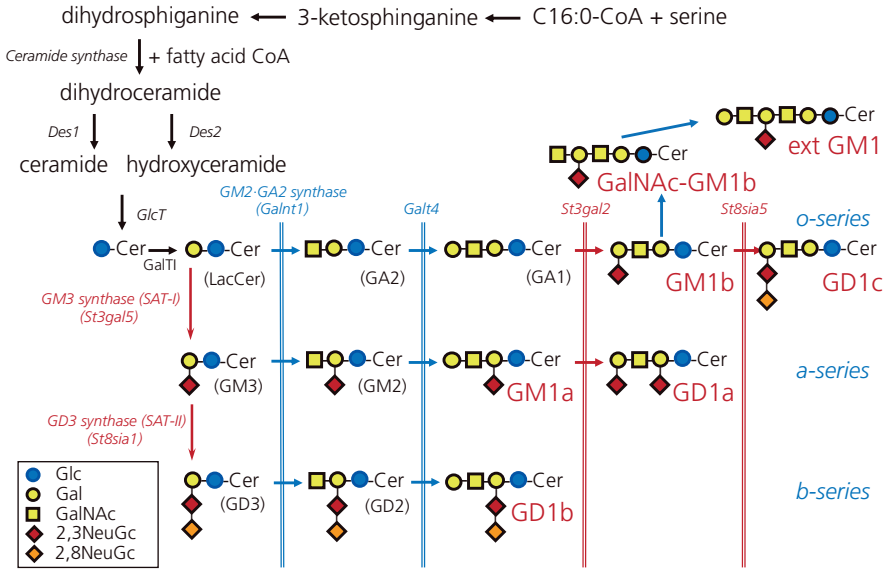

Fig. 1 Metabolic Pathways and Structures of Glycosphingolipids

Only some of the GSLs containing sialic acid, ganglisodes, are shown. Sialic acids are expressed as N-glycolylneuraminic acid (NeuNGc), but because biosynthesis of NeuNGc is deficient in humans, most exist as NeuNAc.

3. Sample Preparation for Structural Analysis of Glycosphingolipids

The lipids were extracted from tissues and cells using 20 volumes of chloroform (C) – methanol (M) (2:1, v/v) equivalent to 20 times that of the sample. If the volume of solvent equivalent to 20 times is too small and insufficient for extraction, a larger volume may be used as appropriate. A glass receptacle, like glass-made centrifugation tubes with caps sealed with a solvent-resistant polymer, must be used for the extraction. After removing the tissue by centrifugation or filter paper, it may be necessary to conduct further extraction using C-M (1:2, v/v) and C-M-water (W) (1:2:0.1, v/v), depending on which SGLs are to be the analytes. To the extract solution obtained with the 20-fold solution of C-M (2:1), add a volume of the water to make the final ratio of C-M-W as 8:4:3, v/v, calculating the volume of tissue derived water as tissue weight. When lightly suspended, a two-phase partition can be obtained. This permits separation of the lipids in the lower layer containing the organic solvent and the salts and hydrophilic low-molecular weight compounds in the upper water/methanol layer. Gangliosides, which consist of relatively long glycans and contain sialic acids, are partitioned to the upper layer. When gangliosides are chosen as the analytes, the upper layer is dried using a nitrogen gas stream or a rotary evaporator, and is then suspended in water and dialyzed against distilled water to remove salts and low-molecular weight compounds. With few exceptions, GSLs of animal origin are resistant to weak alkali, 0.1 N NaOH/methanol is added, and incubated at 40 °C for 2 hours. Then, after neutralization with acetic acid, desalting is conducted by completely drying the mixture, dissolving it in water, and then conducting dialysis. Structural analysis of this sample can then be analyzed by LC-IT-TOF-MS.

Below we present an actual example of analysis of mouse T lymphocyte gangliosides[2]. Thymocytes (1.77×10^9), CD4T cells (1.44×10^8) and CD8T cells (1.27×10^8) were separated using antibodies and magnetic beads, and the lipids were extracted by the method described above. The extract lipids were dissolved in C-M-W (30:60:8), and applied to a DEAE-Sephadex column (acetate form, 2.4 mL column size). After washing unbound substances, acidic fraction was eluted with C-M-1M CH_3COONa (30:60:8). The acidic fraction was dried, and weak alkaline treatment was conducted with 0.1 N NaOH/methanol as mentioned above. After neutralization, dried residues were suspended in water and applied to a Sep-Pak C18 cartridge. After rinsing with water, the ganglioside fraction was obtained using methanol followed by M-C (1:1). The sample was dissolved in methanol, and then subjected to LC-MS analysis.

4. Structural Analysis by LC-IT-TOF-MS

Separation of the ganglioside fraction described above was conducted using reversed phase chromatography with a C30 column, and normal phase chromatography with an NH_2 column, and structural analysis was conducted by LC-IT-TOF-MS. The analytical conditions are presented below.

Analysis using the C30 column: column, Develosil C30-UG-3, 3 µm, 1.0 × 50 mm; solvent A: 10 mM ammonium formate – 0.1 formic acid / 12.5 water / 87.4 methanol v/v; solvent B: 10 mM ammonium formate – 0.1 formic acid / 2.5 water / 49.4 methanol / 50 isopropanol v/v; concentration gradient elution using 0 % B for 5 minutes, 20 minutes to 100 % B, and 100 % B for 5 minutes; flow rate: 50 µL/min.

Analysis using the NH_2 column: column, Unison NH_2, 1.0 × 50 mm; solvent A: 1 mM ammonium formate – 83 acetonitrile / 17 water, v/v; solvent B: 50 mM ammonium formate – 50 acetonitrile / 50 water, v/v; concentration gradient elution using 0 % B for 5 min, 25 min to 76 % B, 5 min to 90 % B; flow rate: 50 µL/min[3].

LC-IT-TOF-MS conditions: the same conditions were used for analysis using both columns. Shimadzu LCMS-IT-TOF; detector voltage: 1.9 kV; CDL: 200 °C; heat block: 200 °C; nebulizer gas: 1.5 L/min; negative mode auto scan: *m/z* 200 – 2000; MS^2 and MS^3 CID energy: 50 %.

Sample injection: Dissolved in 100 µL methanol, 1 – 5 µL injected.

5. Results of Ganglioside Structural Analysis

Fig. 2A – C, and E show the mass chromatograms of gangliosides obtained from thymocytes using the C30 column. Separation was achieved using the structure of ceramides. When a ganglioside structure has 1 unsaturated bond in the fatty residue, it elutes before the ganglioside with 2 fewer carbon chains. This is the relationship between d18:1-24:1 and d18:1-22:0. The elution times of gangliosides with different glycan chains and the same ceramide structures show very small difference, therefore complete separation of each ganglioside is not obtained. A fixed quantity of GM3 (d18:1-14:0) per protein amount is used for ISD, so a relative comparison among gangliosides is possible. However, as the ionization efficiency and detection efficiency vary depending on the structure, it is important to consider the values of peak areas/ISD peal area as a comparative index rather than a quantitative value. In particular, the values obtained by the calculation as peak areas/ISD peak area per mg protein should not be taken as quantitative amount of each ganglioside, but we are able to compare composition values of peak areas/ISD peak area among three cells because the same analytical conditions are used to get the mass chromatograms, giving very important findings. Fig. 2A shows the mass chromatogram for GM1, indicating that the major components are the lipid moieties d18:1-16:0, d18:1-24:1, d18:1-22:0 and d18:1-24:0. GM1 comprises the GM1a and GM1b structural isomers, and in the mouse immune system, synthesis of GM1b is particularly active. So, we conducted separation of GM1a and 1b using an NH_2 column. The results are shown in Fig. 2D. The MS^2 spectral results are shown in Fig. 4A, in which the *m/z* 671.2 fragment derived from the non-reducing terminal is detected only in GM1b, thus permitting the determination of GM1b from the MS^2 mass spectrum. The ratio of GM1a and GM1b can be determined from Fig. 2A and D. The GalNAc-GM1b structure is created when GalNAc is transferred to the Gal terminal of GM1b. The mass chromatogram obtained with the C30 column is shown in Fig. 2B. Lipid moieties having the structures similar to that of GM1 are detected. The C30 mass chromatogram of GD1 is shown in Fig. 2E, however, GD1 exists as a mixture of 3 isomers. GM1b becomes GD1c (NeuNGc-NeuNGc-Gal-GalNAc-Gal-Glc-Cer) with the transfer of sialic acid, and GD1c, GD1b (Gal-GalNAc-(NeuNGc-NeuNGc-)Gal-Glc-Cer) and GD1a (NeuNGc-Gal-GalNAc-(NeuNGc-)Gal-Glc-Cer)

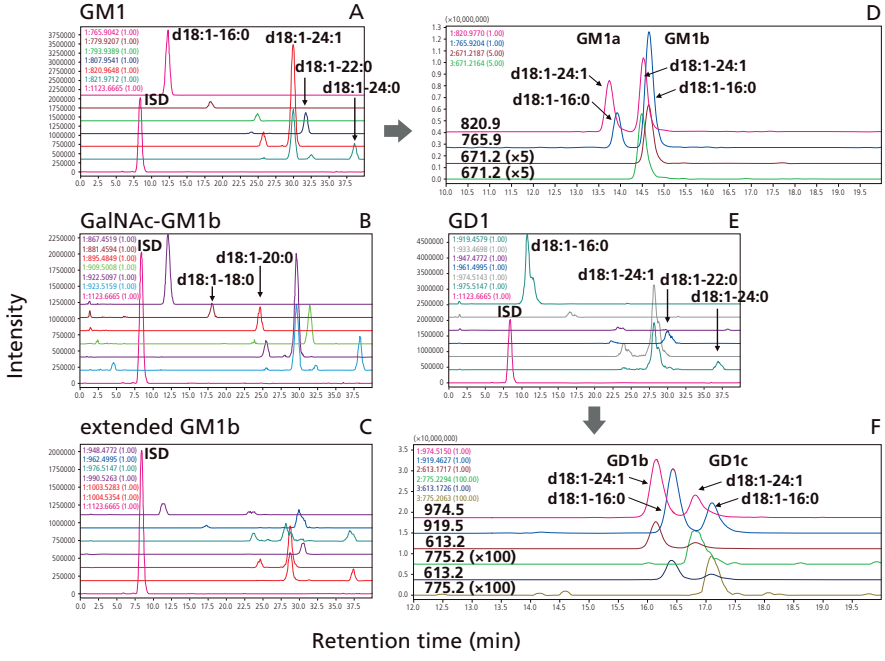

Fig. 2 Analysis of Gangliosides of Mouse Thymocytes by LC-IT-TOF-MS

Mass chromatograms A – C and E were obtained using the reverse phase chromatography with the C30 column, and D and F are normal phase chromatograms obtained with the NH_2 column. Mass chromatogram A shows the detection of GM1. Chromatogram D shows the separation of isomers GM1a and GM1b, B shows the detection of GalNA-GM1b, C shows the detection of extended GM1b, and E shows the detection of GD1. In F, the GD1 isomers are separated into GD1b and GD1c. GM3 (d18:1-14:0) is added as ISD.

This data was reported in the paper titled "CD4 and CD8 T cells require different membrane gangliosides for activation", Nagafuku M, Okuyama K, Onimaru Y, Suzuki A, Odagiri Y, Yamashita T, Iwasaki K, Fujiwara M, Takayanagi M, Inokuchi J (2012) *Proc. Natl. Acad. Sci. U.S.A.* 109, E336–E342.

are present. Here, the sialic acid is NeuNGc. In the mouse immune tissues, NeuNGc is strongly expressed due to the activation of CMP-NeuNAc hydroxylase. As shown in Fig. 2F, separation of GD1b and GD1c is possible with the NH_2 column, and the content of GD1a, b and c can be understood from E and F. This distinction of these three molecules also can be made from the MS^2 spectrum, which will be discussed later.

Fig. 3 shows the comparison of thymocytes, CD4T cells and CD8T cells based on the mass chromatograms obtained with the C30 column. The ISD ratio makes it possible to understand the differences among the cells in terms of ganglioside content. It is clear that GalNAc-GM1b and extended GM1b are significantly increased in the CD8T cells. At the same time, there is a marked increase in the molecules containing the d18:1-24:1, d18:1-22:0 and d18:1-24:0 ceramide structures. As for the CD4T cells, there is a greater percentage of GD1 than CD8T cells, and although close to thymocytes, the d18:1-22:0, d18:1-24:0 percentage is greater. These changes are of interest with respect to cell differentiation, the resulting functional differentiation.

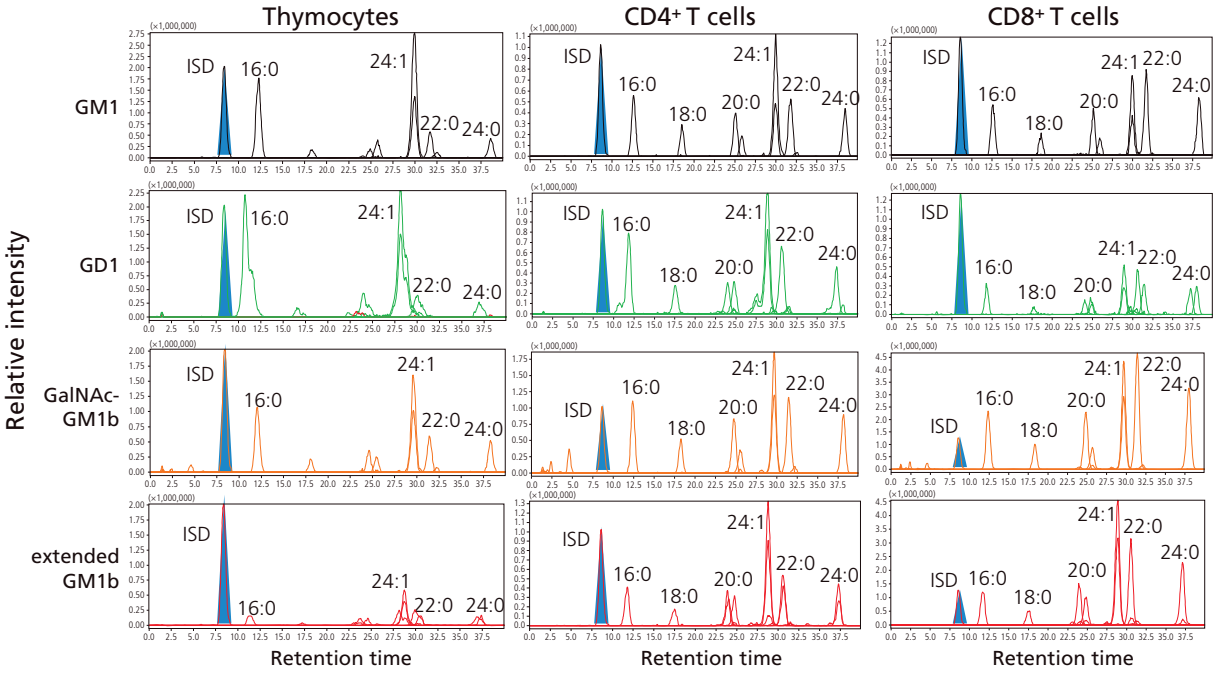

Fig. 3 Mass Chromatograms Obtained from Analysis of Gangliosides of Thymocytes, CD4T Cells and CD8T Cells Using the C30 Column

GM3 (d18:1-14:0) as ISD is added in an amount corresponding to the amount of protein, thereby permitting a comparison of the relative amounts of gangliosides among the cells.

This data was reported in the paper titled "CD4 and CD8 T cells require different membrane gangliosides for activation", Nagafuku M, Okuyama K, Onimaru Y, Suzuki A, Odagiri Y, Yamashita T, Iwasaki K, Fujiwara M, Takayanagi M, Inokuchi J (2012) *Proc. Natl. Acad. Sci. U.S.A.* 109, E336–E342.

Fig. 4 shows the MS^2 spectra from the viewpoint of positional isomer distinction. Fig. 4A shows the spectra of GM1a and GM1b. Both of these were detected as $[M - 2H]^{-2}$ due to the presence of NeuNGc, while GM1a containing NeuNAc was detected as $[M - H]^-$ under the same analytical conditions. The MS^2 analysis detected the ion at *m/z* 306.1 derived from NeuNGc, at 851.3 from NeuNGc-Gal-GalNAc-Gal or Gal-GalNAc-(NeuNGc-)Gal, at 970.7 from Gal-Glc-Cer(d18:1-24:1), and at 1335.8 from Gal-GalNAc-Gal-Glc-Cer(d18:1-24:1). Further, the structure-specific ions *m/z* 486.1 derived from NeuNGc-Gal and *m/z* 671.2 derived from NeuNGc-Gal-GalNAc are detected only in GM1b. Both can be used to determine the structure of ceramide in MS^3 analysis with the *m/z* 646.6 precursor. Fig. 3B is an MS^2 spectrum obtained using the $[M - 2H]^{-2}$ precursor ion of GD1b and GD1c. Ions in common were detected at *m/z* 306.1 derived from NeuNGc, *m/z* 613.1 from NeuNGc-NeuNGc, *m/z* 970.7 from Gal-Glc-Cer, *m/z* 1335.8 from Gal-GalNAc-Gal-Glc-Cer, and *m/z* 1642.9 from Gal-GalNAc-(NeuNGc-)Gal-Glc-Cer or NeuNGc-Gal-GalNAc-Gal-Glc-Cer), respectively. A GD1b-specific ion derived from NeuNGc-NeuNGc-Gal is detected at *m/z* 775.2. Fig. 4C shows the MS^2 spectrum obtained from $[M - 2H]^{-2}$ as a precursor ion of GalNAc-GM1b. Characteristic ions were detected at *m/z* 689.2 and *m/z* 874.3. Fig. 4D shows the MS^2 spectrum of the $[M - 2H]^{-2}$ precursor ion of Gal-GalNAc-GM1b (extended GM1b). The fragment ions at *m/z* 365.3 derived from Gal-GalNAc, *m/z* 851.2 from Gal-GalNAc-(NeuNGc-)Gal + H_2O, and *m/z* 1036.3 from Gal-GalNAc-(NeuGc-)Gal-GalNAc are characteristic.

As described above, sugar chain structure information was obtained for each ganglioside to permit identification, but the structure of the ceramide must be identified at the same time. It is possible to assume the structure from the retention time obtained by the C30 column, but identification of sphingosine and the fatty acids is required. In most tissues and cells, the main constituent is d18:1 sphingosine (C18 sphingenine), but in neurons, there is a large amount of d20:1 sphingosine, while in myelin, there are 24:0, h24:0, 24:1, h24:1 fatty acids, and in digestive tract epithelial cells, there are t18:0 and hydroxyl fatty acids. Cermide structures are tissue-specific. It has already been mentioned that specific ceramide structures are is present in the skin. Fig. 4E shows the MS^3 spectrum of ceramide at *m/z* 646.6 as the precursor obtained from MS^2 of *m/z* 1003.5, the divalent Gal-GalNAc-(NeuGc-)Gal-GalNAc-Gal-Glc-Cer ion. Annotation of the fragment ions have already been reported, and those results are shown to the right of Fig. 4F. Although the P ion (*m/z* 237.2) was not detected, detection of the other ions permitted identification of the ceramide structure as being d18:1-24:1.

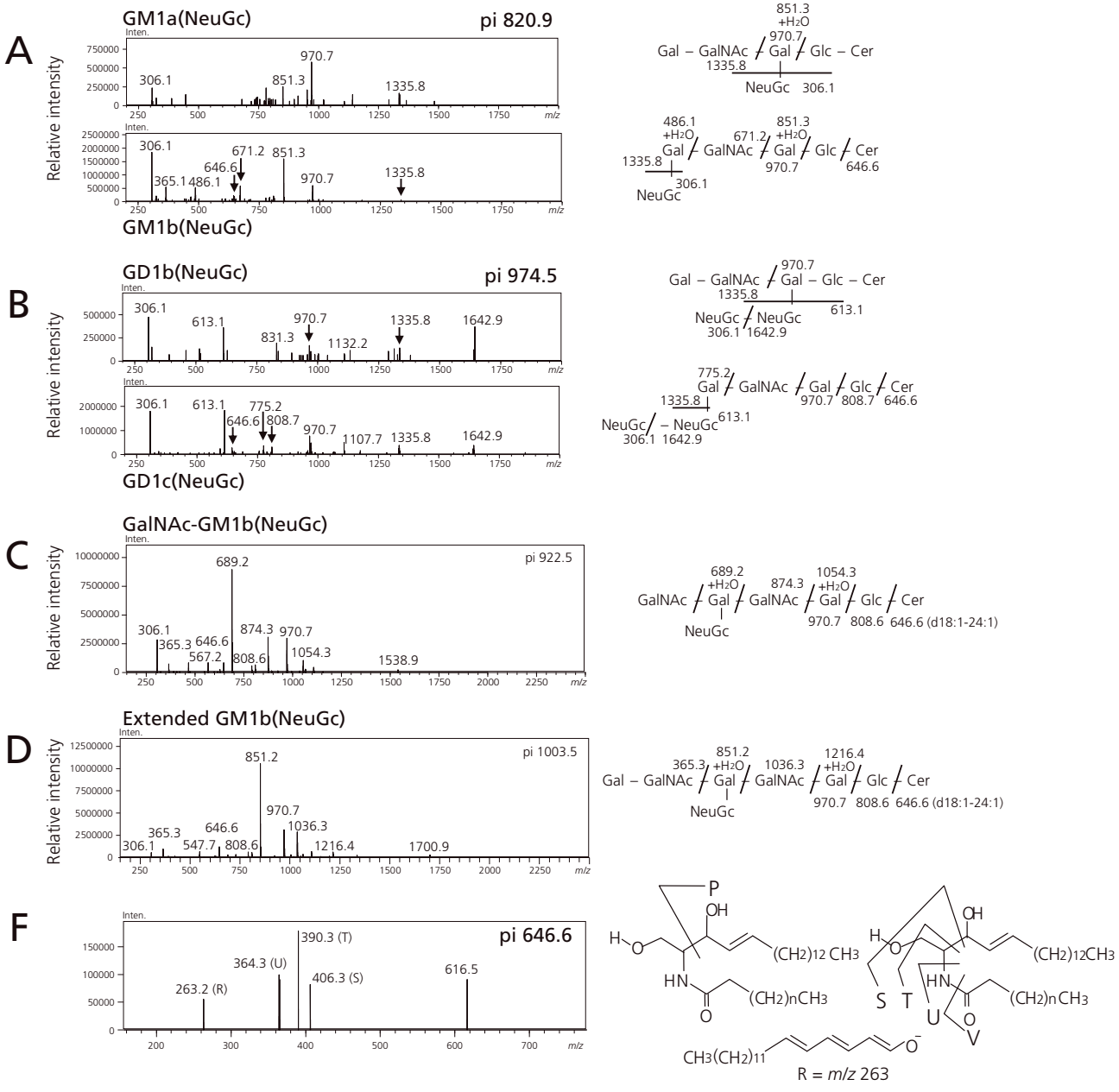

Fig. 4 MS² Spectra of Gangliosides GM1a, GM1b, GD1b, GD1c, Ga1NAc-GM1b, and Extended GM1b. MS³ Spectrum of Extended GM1b.

All of the sialic acids are NeuNGc. The distinctions between GM1a and GM1b (in A), and GD1b and GD1c (in B) are shown respectively. The characteristic fragmentation ions of Ga1NAc-GM1b (in C) and extended GM1b (in D) are shown. The MS³ spectrum of the 646.6 extended GM1b precursor ion (E) can be used to verify that the ceramide structure is d18:1-24:1.

This data was reported in the paper titled "CD4 and CD8 T cells require different membrane gangliosides for activation", Nagafuku M, Okuyama K, Onimaru Y, Suzuki A, Odagiri Y, Yamashita T, Iwasaki K, Fujiwara M, Takayanagi M, Inokuchi J (2012) *Proc. Natl. Acad. Sci. U.S.A.* 109, E336–E342.

Table 1 Gangliosides Collected Using MS^2, MS^3 Spectra

GM3(d16:1-23:0)	GM2(G,d18:0-h16:0)	GD1a(d18:0-18:0)	GQ1b(d18:0-18:0)
GM3(d18:0-16:0)	GM2(G,d18:1-15:0)	GD1a(d18:1-16:0)	GQ1b(d18:1-18:0)
GM3(d18:1-16:0)	GM2(G,d18:1-16:0)	GD1a(d18:1-18:0)	GQ1b(d18:1-22:0)
GM3(d18:1-18:0)	GM2(G,d18:1-18:0)	GD1a(d18:2-18:0)	GQ1b(d20:1-18:0)
GM3(d18:1-20:0)	GM2(G,d18:1-20:0)	GD1a(d20:0-18:0)	GT1b(d18:1-18:0)
GM3(d18:1-22:0)	GM2(G,d18:1-22:0)	GD1a(d20:1-18:0)	GT1b(d20:1-18:0)
GM3(d18:1-23:0)	GM2(G,d18:1-23:0)	GD1b(d18:0-18:0)	OAc-GD1b(d18:1-18:0)
GM3(d18:1-24:0)	GM2(G,d18:1-24:0)	GD1b(d18:1-18:0)	OAc-GD1b(d20:1-18:0)
GM3(d18:1-24:1)	GM2(G,d18:1-24:1)	GD1b(d18:1-23:0)	OAc-GD1b(d20:1-20:0)
GM3(d18:1-h24:0)	GM2(G,d18:1-24:2)	GD1b(d20:1-18:0)	OAc-GQ1b(d18:1-18:0)
GM3(d18:1-h24:1)	GM1a(G,d18:1-16:0)	GD1b(d20:1-20:0)	OAc-GQ1b(d20:1-18:0)
GM3(d18:2-h18:0)	GM1a(G,d18:1-18:0)	GD3(d18:1-18:0)	OAc-GT1b(d18:1-18:0)
GM3(d20:1-h22:0)	GM1a(G,d18:1-20:0)	GD3(d18:1-20:0)	OAc-GT1b(d20:1-18:0)
GM3(G,d18:1-16:0)	GM1a(G,d18:1-22:0)	GD3(d18:1-22:0)	diOAc-GQ1b(d18:1-18:0)
GM3(G,d18:1-18:0)	GM1a(G,d18:1-23:0)	GD3(d18:1-23:0)	diOAc-GQ1b(d20:1-18:0)
GM3(G,d18:1-20:0)	GM1a(G,d18:1-24:0)	GD3(d18:1-24:0)	
GM3(G,d18:1-22:0)	GM1a(G,d18:2-24:1)	GD3(d18:1-24:1)	
GM3(G,d18:1-23:0)	GM1b(d18:1-16:0)	GM1(d18:1-24:1)	
GM3(G,d18:1-24:0)	GM1b(d18:1-22:0)	GM1(d18:1-16:0)	
GM3(G,d18:1-24:1)	GM1b(d18:1-23:0)	GM1(d18:1-18:0)	
GM4(d18:1-24:1)	GM1b(d18:1-24:0)	GM1(d18:2-18:0)	
GM2(d18:0-h18:0)	GM1b(G,d18:1-16:0)	GM1(d20:1-18:0)	
GM2(d18:1-16:0)	GM1b(G,d18:1-22:0)	GM1a(d18:1-23:0)	
GM2(d18:1-18:0)	GM1b(G,d18:1-23:0)	GM1a(d18:1-24:1)	
GM2(d18:1-h18:0)	GM1b(G,d18:1-24:0)	GM1a(d18:2-24:1)	
GM2(G,d18:0-16:0)	GM1b(G,d18:1-24:1)		
	GM1b(G,d18:1-24:2)		

6. Tools for Structural Analysis

Among the analysis examples described above, those for GD1 and GM1 have already been reported[3, 4]. The analysis methods utilized here were already reported, but the results for gangliosides containing NeuNGc as well as for GalNAc-GM1b and Gal-GalNAc-GM1b were reported for the first time[2]. Acquiring the MS^2 and MS^3 spectra and analyzing the fragmentation requires a great deal of effort, and therefore requires robust computer-automated analysis and data mining procedures, indicating requirement of a database containing mass spectra and a search engine that can utilize it. We are currently compiling mass spectra with the aim of achieving both of these goals, and the list of glycolipids already sampled is shown in Table 1. Once identification of the GSLs becomes possible, analysis of quantitative changes based on spectra will be essential for functional analysis. This requires MRM (multiple reaction monitoring) utilizing a triple stage quadrupole MS measurement system, and suitable internal standards. When utilizing a sequential analytical system becomes possible, such systems will be applicable to many projects, such as the functional analysis of GSLs, analysis of their relationship to diseases, observation of the course of disease states, and development of therapeutic products, etc., with the expectation of accelerated research promotion.

7. Future Analysis of Glycolipids

Here we discuss the future subjects of the authors' interests in the research fields of GSLs, especially related to GSL functions Using the diabetes model mice and glycosyltransferase gene knockout mice, Inoguchi et al. demonstrated the possibility that insulin receptor (IR) function may be controlled by GM3 (NeuAcα3Galβ4GlcβCer) in the cell membrane. The authors proposed the hypothesis that insulin signals are transmitted only when IRs interact with caveolins, the IR-GM3 complex is formed as GM3 in the cell membrane becomes more abundant, and insulin signals are not transmitted because IRs are excluded from the microdomains in which IR-caveolin interaction occurs[5]. It would become an issue in the treatment of type II diabetes, if we are able to manipulate the presence of GM3 in the mcrodomains. Yanagisawa et al. at, Japan's National Center for Geriatrics and Gerontology, who are conducting research on the molecular mechanism of amyloid β (Aβ) aggregation which causes Alzheimer's disease, reported that the aggregation is triggered with the seeding of GM1[6]. It has been demonstrated in in vitro analysis that GM1 specifically enhances the aggregation of Aβ. If this trigger mechanism can be elucidated, controlling the state of existence of GM1 may slow down the development of the disease or delay the onset of the disease. It has been shown that deposition of α-synuclein is one of the causes of Parkinson's disease, and it has been indicated that the risk of Parkinson's disease incidence is heighted in individuals having a heterozygous gene mutation of β-galactosidase, which degrades GlcβCer. It is supposed that a decrease in the enzyme activity causes a change in the levels of GlcβCer in the membrane, resulting in a change of the membrane microdomain and an increase in deposition of α-synuclein[7]. In other diseases as well, it is possible to imagine that membrane microdomains are involved. If the progression of the diseases can be slowed by somehow adjusting conditions in the microdomains, this could lead to the development of new direction of disease treatments. An important physiological function of ceramide, GlcβCer and acylglucosylceramide in the skin is the formation of a water barrier. Ceramide is already being used in cosmetics, but the biosynthesis of these specific GSLs, their regulation and their relationship to epidermal cell differentiation remain to be elucidated. There is a wide gulf between conducting structural analysis of GSLs and establishing a quantitation method for such trace levels, but we have just gained a clue for this.

References

1. Simons K, Ikonen E (1997) *Nature* 387, 569–572
2. Nagafuku M, Okuyama K, Onimaru Y, Suzuki A, Odagiri Y, Yamashita T., Iwasaki K, Fujiwara M, Takayanagi M, Inokuchi J (2012) *Proc. Natl. Acad. Sci. U.S.A.* 109, E336–E342
3. Ikeda K, Taguchi R (2010) *Rap. Commun. Mass Spectrom.* 24, 2957–2965
4. Ikeda K, Shimizu T, Taguchi R (2008) *J. Lipid Res.* 49, 2678–2689
5. Kabayama K, Sato T, Saito K, Loberto N, Prinetti A, Sonnino S, Kinjo M, Igarashi Y, Inokuchi J (2007) *Proc. Natl. Acad. Sci. U.S.A.*, 104, 13678–13683
6. Yanagisawa K, Odaka A, Suzuki N, Ihara Y. (1995) *Nat Med.* 1, 1062–1066
7. Mazzulli J R, Xu Y-H, Sun Y, Knight A L, McLean P J, Caldwell G A, Sidransky E, Grabowski G A, Krainc D. (2011) *Cell* 146, 37–52

First Edition: September, 2014

SHIMADZU

Shimadzu Corporation

www.shimadzu.com/an/

Printed in Japan 3655-07430-10ANS